



# THE VARIATIONAL PROJECTION METHOD: A NEW TECHNIQUE TO SIMULATE THE SEISMIC RESPONSE OF SHALLOW ALLUVIAL VALLEYS

F.J. SÁNCHEZ-SESMA, K. IRIKURA<sup>1</sup>, J. PERROT,  
J.L. RODRÍGUEZ-ZÚÑIGA<sup>2</sup> AND R. AVILA-CARRERA

Instituto de Ingeniería UNAM,  
Del. Coyoacán, 04510 México D.F., México.

1-Disaster Prevention Research Institute, Kyoto University.

2-Centro de Investigación Sísmica A C, México D.F.

## ABSTRACT

We present a new method: the Variational Projection Method (VPM) to compute the seismic response of three-dimensional (3-D) shallow alluvial valleys. Our approach is based on a weak-form variational Galerkin formulation of the problem for a smooth irregular layer overlaying an elastic half-space. The Galerkin method is applied using a simple set of trial functions for depth dependence. The coupled partial differential equations of dynamic elasticity in space and time are "projected" into the horizontal plane and are then solved using a pseudospectral scheme: finite differences in time and FFT to compute spatial horizontal derivatives.

Examples are given of the numerical performance and accuracy of the VPM for 3-D alluvial basin model. Our method appears to be fast and accurate. The VPM has been applied to compute the ground motion at some locations in Osaka, Japan, during the January 17, 1995 Hyogo-ken Nambu (Kobe) earthquake considering the response of the basin (Perrot *et al.*, 1995). This approach is being used to simulate the seismic response of Mexico City Valley and to study azimuthal effects (Rodríguez-Zúñiga and Sánchez-Sesma, 1996).

## KEYWORDS

Alluvial Valleys; Seismic Response; Variational projection; 3D irregular valley; Mexico City Valley; January 17, 1995 Kobe earthquake, Japon.

## INTRODUCTION

Local site effects can produce large spatial variations of seismic ground motion and concentrated damage. In the last three decades significant efforts have been devoted to the characterization of such effects (for reviews see Sánchez-Sesma, 1987; Aki, 1988; Luco *et al.*, 1990). The great importance of local amplification was again confirmed after the damage produced in various recent earthquakes. For instance, Mexico City in 1985, San Francisco in 1989 and, more recently, Kobe in 1995.

The physical basis of the site amplification problem are now well understood. Most of the research effort has been concentrated on 2-D problems. This has allowed some explanation to observations. However, in order to improve the quantitative account of site response, modeling should consider the 3-D nature of the problem. For instance, the spatial variability and polarization of observed ground motion in Mexico City have been interpreted as 3-D effects (Pérez-Rocha *et al.*, 1991; Sánchez-Sesma *et al.*, 1993).

Several methods have been proposed to study the propagation of seismic waves in 3-D alluvial valleys (for a recent review see Sánchez-Sesma and Luzón, 1995). The boundary element method (BEM) allows to get reliable results useful both for understanding and to calibrate other procedures. In some circumstances, a BEM analysis is warranted to have a glimpse of 3-D effects of simplified configurations. However, it is restricted by the availability of Green's functions for heterogeneous media. Finite elements and finite differences allow for heterogeneity of materials and can handle virtually any geometrical configuration. In fact, the most realistic simulations to date are those of finite differences. The study by Frankel (1993) on the response of the San Bernardino Valley, California, to nearby earthquakes and the recent simulations by Olsen *et al.* (1995), for the Los Angeles basin illustrate well this fact. However, although these results are encouraging, modeling lags behind reality. Moreover, trustworthy simulations can be very difficult, even with supercomputers. Therefore, we believe there is a lack of simplified, practical procedures to account for site effects in shallow alluvial basins.

In this work, a new method is presented to approximately simulate the seismic response of 3-D shallow alluvial basins. Our approach attempts to overcome the mentioned difficulties. To design it we began by taking into account the fine structure observed in the frequency response of 2-D models of shallow alluvial valleys (Sánchez-Sesma *et al.*, 1993) which evince a strong coupling between 1-D response and locally generated surface waves in this type of configurations. To this end, we proposed an experimental approach using local mode expansion (Avila-Carrera *et al.*, 1993). On the other hand, variational formulations of the type pioneered by Galerkin, which provide efficient, accurate formulations for wave propagation problems (Martínez and Bielak, 1980; Faccioli *et al.*, 1996), give also a framework to our quest. Galerkin weak-form formulation is also the basis of a recent rigorous method in the frequency domain called Direct Solution Method (DSM) (Geller *et al.*, 1990; Geller and Ohminato, 1994; Geller and Hatori, 1995). Geller and coworkers are solving a set of problems of seismological interest with high accuracy.

Therefore, in order to exploit the much larger lateral extension of the problem we use a weak-form variational formulation and locally apply Galerkin method in order to "project" the field equations of dynamic elasticity into the horizontal plane. We use complete sets of trial functions for depth dependence. Therefore, our Variational Projection Method (VPM) produces a set of "projected" equations in which the dependence of horizontal coordinates and time is preserved. These equations are then solved with a pseudospectral method: time derivatives are approximated with a centered leap-frog scheme, while spatial derivatives are obtained using Fourier transforms. We apply this procedure for the soft sediments and assume a smooth variation of the interface. The problem can be formulated in two ways: (1) by specifying the motion at the interface (using both ray theory and Haskell method) which means that late reflections will correspond to rigid basement and thus energy loss by radiation into the exterior medium can be accounted for only approximately with time operators and (2) by (additionally) specifying some stresses at the interface in terms of partially reflecting boundaries. These two ways give encouraging results, but to establish which is the best one is a matter of current research. Our formulation appears to be much faster than the existing procedures.

We give some examples of the numerical performance and accuracy of the VPM for 2-D and 3-D alluvial basin models. The VPM has been applied to compute the ground motion at some locations in Osaka, Japan, during the January 17, 1995 Hyogo-ken Nanbu (Kobe) earthquake considering the response of the basin for a point dislocation source (Perrot *et al.*, 1995). This approach is being used to simulate the seismic response of Mexico City Valley and to study azimuthal effects (Rodríguez-Zúñiga and Sánchez-Sesma, 1996).

## VARIATIONAL PROJECTION METHOD

### Formulation of the Problem

Consider a shallow 3-D alluvial valley on the surface of an elastic half-space. The material of the sediments is elastic and have a smooth but otherwise arbitrary shape described by the thickness  $h(x, y)$ . We also assume that the sediments are much softer than the underlying half-space.

The field equations in absence of body forces can be written for the sediments by means of Newton's Law:

$$\frac{\partial \sigma_{ij}}{\partial x_j} = \rho \frac{\partial^2 u_i}{\partial t^2}, \quad i = 1, 2, 3 \quad (1)$$

where  $\sigma_{ij}$  is the stress tensor,  $u_i$ , the displacement vector,  $x_i$ , the cartesian coordinates,  $\rho$ , the mass density and  $t$ , the time. We may use in what follows the equivalences  $x_1 = x$ ,  $x_2 = y$ ,  $x_3 = z$  and  $u_1 = u$ ,  $u_2 = v$ ,  $u_3 = w$ . For the sake of completeness, the stress tensor is given by Hooke's Law :

$$\sigma_{ij} = c_{ijkl} \frac{\partial u_k}{\partial x_l}, \quad (2)$$

where  $c_{ijkl}$  is the elastic tensor (For isotropic materials we have  $c_{ijkl} = \lambda \delta_{ij} \delta_{kl} + \mu (\delta_{ik} \delta_{jl} + \delta_{il} \delta_{jk})$ ). Let us assume the elastic displacement field in the sediments with the form

$$u_i(x, y, z, t) = u_i^{(0)}(x, y, h, t) + u'_i(x, y, z, t) \quad (3)$$

where  $u_i^{(0)}$  is a known reference motion at the interface  $h(x, y)$  and  $u'_i$  is the additional motion in the layer we are looking for. Substituting Eq. 3 into Eqs. 2 and 1, one may write:

$$\frac{\partial \sigma'_{ij}}{\partial x_j} + f_i = \rho \frac{\partial^2 u'_i}{\partial t^2} \quad (4)$$

where

$$f_i = \frac{\partial \sigma_{ij}^{(0)}}{\partial x_j} - \rho \frac{\partial^2 u_i^{(0)}}{\partial t^2} \quad (5)$$

is the driving field due to the reference motion  $u_i^{(0)}$ .

The stress-free boundary conditions at  $z = 0$  is then

$$\sigma_{zj} = \sigma_{zj}^{(0)} + \sigma'_{zj} = 0 \quad (6)$$

Notice that  $\sigma_{zj}^{(0)}$  depends only on  $x$ ,  $y$  and  $t$ . Let us write the seek displacement field by means of :

$$u'_i(x, y, z, t) = \sum_{n=1}^N U_i^n(x, y, t) \varphi^n(z) \quad (7)$$

where  $U_i^n$  are functions of horizontal coordinates  $(x, y)$  and time while  $\varphi^n(z)$  are given trial functions of depth. Eq. 7 express the solution  $u'_i$  in terms of a linear combination of trial functions.

### Weak-form of Galerkin Formulation

Consider now, the Galerkin strong-form operator,

$$\int_0^h \left[ \frac{\partial \sigma'_{ij}}{\partial x_j} + f_i - \rho \frac{\partial^2 u'_i}{\partial t^2} \right] \varphi^m(z) dz = 0 \quad (8)$$

Equation 8 together with Eq. 6 can be seen as the strong-form of the Galerkin method for the elastic equations along a vertical line with length  $h(x, y)$ . To express Eq. 3 in the form of a weak-form operator we integrate by parts and write

$$\int_0^h \left\{ \left[ \frac{\partial \sigma'_{xi}}{\partial x} + \frac{\partial \sigma'_{yi}}{\partial y} + f_i - \rho \frac{\partial^2 u'_i}{\partial t^2} \right] \varphi^m(z) - (\sigma'_{zi} + \sigma_{zi}^{(0)}) \frac{d\varphi^m}{dz} \right\} dz + [(\sigma'_{zi} + \sigma_{zi}^{(0)}) \varphi^m(z)]_0^h = 0 \quad (9)$$

because  $\sigma_{zi}^{(0)}$  has no dependence on  $z$ . According to Eq. 6, the only contribution of the last term in Eq. 3 comes from  $z = h$  if  $\varphi^m(h) \neq 0$ .

## The Projected Equations

If  $\varphi^m(h) = 0$ , then  $u'_i(x, y, h, t) = 0$  and the reference motion  $u_i^{(0)}$  could be considered the actual motion of the interface. If these motions are given and correspond to the 1-D solution at the interface, the solution at early times of response would effectively agree with the condition  $u'_i = 0$  at  $z = h$ . For later times the boundary is totally reflecting and corresponds to a rigid base.

Among various possible sets of complete functions for the interval  $(0, h)$  we selected the well known set of cosines:

$$\varphi^n(z) = \cos \lambda_n z \quad (10)$$

with  $\lambda_n = (2n + 1)\pi/2h$ . It is clear that  $\varphi^m(h) = 0$ . Moreover, these functions and their derivatives (with respect to  $z$ ) form, respectively, orthogonal sets in the interval of interest. These properties are useful to simplify the "projection" of the field equations of dynamic elasticity into the horizontal plane.

Introducing Eq. 7 into Eq. 9, considering Eqs. 2 and 3 and taking into account that even if  $h$  is function of  $x$  and  $y$ , the corresponding derivatives of  $h$  are neglected, we can write:

$$\begin{aligned} U_{tt}^m - \alpha^2 U_{xx}^m - \beta^2 U_{yy}^m + \beta^2 \lambda_m^2 U^m - (\alpha^2 - \beta^2 V_{xy}^m - ((\alpha^2 - 2\beta^2)a_{mn} - \beta^2 a_{mn})) W_x^n \frac{2}{h} \\ = \frac{1}{\rho} f_1 \frac{4}{\pi} \frac{(-1)^m}{2m+1} + \frac{2}{\rho h} \sigma_{zz}^{(0)} \end{aligned} \quad (11)$$

$$\begin{aligned} V_{tt}^m - \beta^2 V_{xx}^m - \alpha^2 V_{yy}^m + \beta^2 \lambda_m^2 V^m - (\alpha^2 - \beta^2 U_{xy}^m - ((\alpha^2 - 2\beta^2)a_{mn} - \beta^2 a_{mn})) W_y^n \frac{2}{h} \\ = \frac{1}{\rho} f_2 \frac{4}{\pi} \frac{(-1)^m}{2m+1} + \frac{2}{\rho h} \sigma_{zy}^{(0)} \end{aligned} \quad (12)$$

$$\begin{aligned} W_{tt}^m - \beta^2 W_{xx}^m - \beta^2 W_{yy}^m + \alpha^2 \lambda_m^2 W^m + ((\alpha^2 - 2\beta^2)a_{nm} - \beta^2 a_{nm}) [U_x^n + V_y^n] \frac{2}{h} \\ = \frac{1}{\rho} f_3 \frac{4}{\pi} \frac{(-1)^m}{2m+1} + \frac{2}{\rho h} \sigma_{zz}^{(0)} \end{aligned} \quad (13)$$

which is a "projected" set of coupled partial differential equations. Here  $U_1^n = U^n$ ,  $U_2^n = V^n$  and  $U_3^n = W^n$  and the subscripts of  $U$ ,  $V$  and  $W$  mean partial derivatives. The spatial derivatives are computed using the Fourier transform by means of the FFT algorithm. The matrix  $a_{mn}$  results from the integral of  $\varphi^n(z)$  and the derivative of  $\varphi^n(z)$ .

It may be verified that the coupling between horizontal functions between various orders comes after the first "variational" derivative with respect to  $z$ . On the other hand, the second derivative of, say,  $U^m$  with respect to  $z$  is given by the product  $-\lambda_m^2 U^m$ .

In order to introduce damping, the easiest way is to adopt the operator  $\frac{\partial}{\partial t} + \gamma$  instead of the time derivative. For instance, under this assumption, the second derivative  $U_{tt}^n$  may read

$$U_{tt}^n = \frac{\partial^2 U^n}{\partial t^2} + 2\gamma \frac{\partial U^n}{\partial t} + \gamma^2 U^n \quad (14)$$

and discretized at time  $j$  we have

$$(U_{tt}^n)^j = \left[ \left( 1 + \gamma \Delta t + \frac{1}{2} \gamma^2 \Delta t^2 \right) U^{n,j+1} - 2U^{n,j} + \left( 1 - \gamma \Delta t + \frac{1}{2} \gamma^2 \Delta t^2 \right) U^{n,j-1} \right] \Delta t^{-2} \quad (15)$$

It can be shown that  $\gamma \simeq \pi f_p / Q$  for a quality factor  $Q$  in the neighborhood of the frequency  $f_p$ . From Eq. 15 and its equivalences for  $V_{tt}$  and  $W_{tt}$  it is possible to compute the functions  $U$ ,  $V$  and  $W$  at the horizontal grid points at time  $j+1$  as a function of values at time  $j-1$  and spatial derivatives at time  $j$ .

The computation of horizontal derivatives is accomplished conveniently with the FFT algorithm using *all* the grid points in a centered scheme. This pseudospectral approach requires at least between 2 and 3 grid-points per wavelength (finite differences may require 8 points to provide similar accuracy). A recent account of pseudospectral techniques can be found in Faccioli *et al.* (1996).

Finally, Eqs. 3 and 7 allow to compute the surface displacements.

## SYNTHETICS FOR A 3D IRREGULAR VALLEY

In order to test the accuracy of the VPM, we make synthetics for a 3D irregular Valley and compared these results with those obtained by Sánchez-Sesma and Luzón (1995) with the IBEM method. The 3D geometry of the interface which limits the sediments (region  $R$ ) from the basement (region  $E$ ) is described in Sánchez-Sesma F.J. and Luzón (1995). The  $S$  wave velocity of the sediments and half-space are  $\beta_R=1$  km/s and  $\beta_E=2.5$  km/s, respectively, the Poisson coefficients are  $\nu_R=0.35$  and  $\nu_E=0.25$  and the densities are related by  $\rho_R=0.8\rho_E$  where  $\rho_E$  is the density of the basement. The quality factor in the basin is  $Q=100$ .

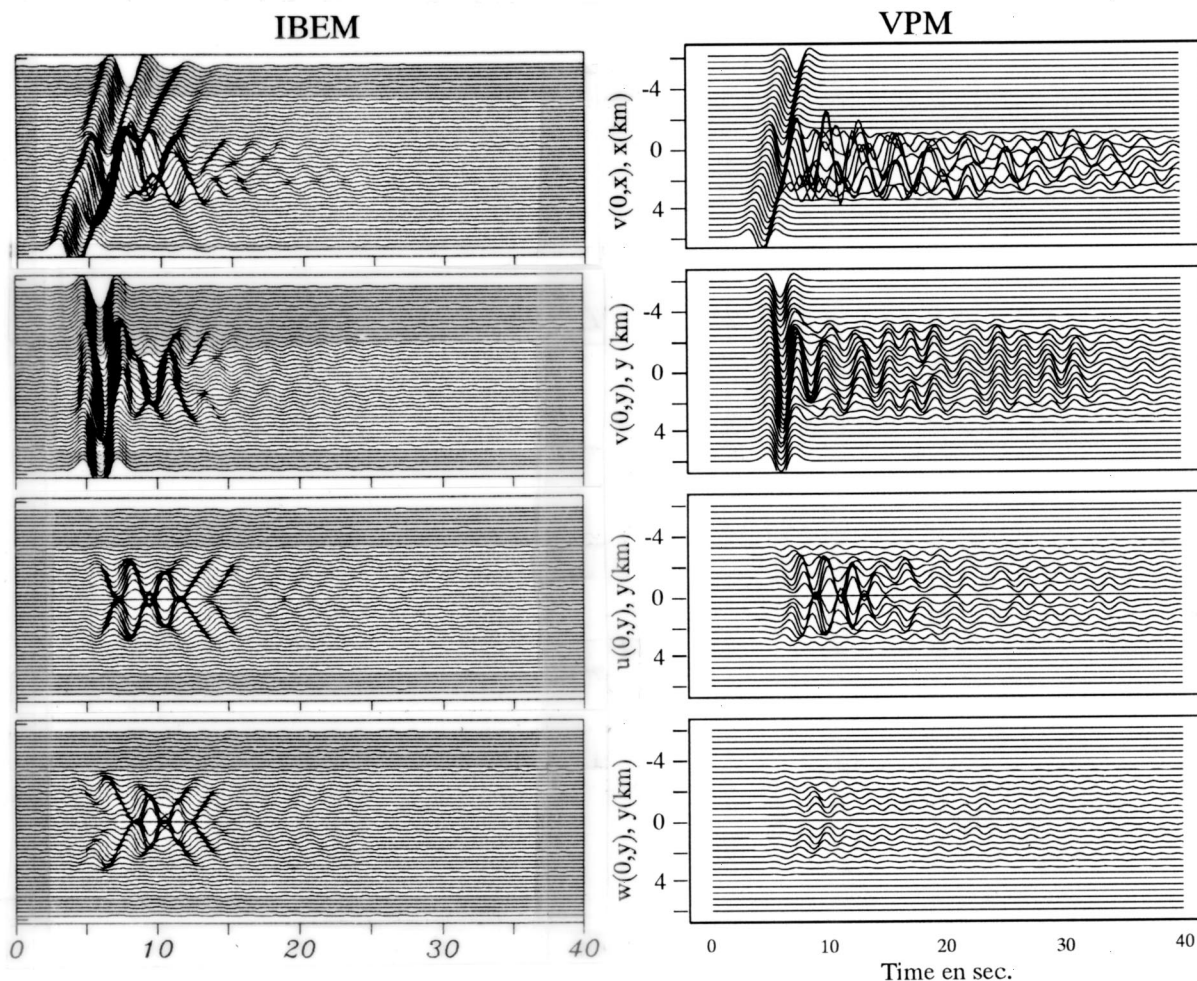


Fig. 1: Comparison between the IBEM method on the right and the VPM one, on the left. These synthetics are calculated for a SH wave of  $\gamma = 30^\circ$  and for different profiles.

We present the results (Figure 1) obtained for an  $SH$  wave with an incidence angle of  $\gamma = 30^\circ$ . We assume for the incoming wave a Ricker wavelet with a characteristic period  $t_p = 3$  sec. We obtained a good simulation in time and amplitude of the first arrivals for each profile. The very high amplitude which arrives on the component  $v(0,x)$  along the  $x$ -profile just after the first arrival for the IBEM method is also well represented on the same profile using the VPM method. But some waves which arrive and are present 5 sec after the first arrival for the IBEM method are not present on the results of the VPM. The profiles obtained with the VPM show also a lot of noise during all the 40 sec of the synthetics. All these problems are consequence of the "rigid base" assumption. They could probably be reduced using reflecting-absorbing boundary conditions. It is a subject of our current research.

## GROUND MOTIONS AT OSAKA DURING 1995 KOBE EARTHQUAKE

The VPM has been applied to simulate the ground motion at Osaka stations during the January 17, 1995 Kobe, Japan, earthquake. This event ( $M_w = 6.9$ ) originated at the very edge of Osaka Bay just beneath the city of Kobe. The small hypocentral distance, probable source directivity effects and

impressive site amplifications account for the unprecedented damage to the city. We do not attempt to deal here with the ground motion at Kobe itself but concentrate instead into the response of the large Osaka basin. Our aim is to interpret the ground motion recorded at some sites in Osaka which clearly show the influence of the deep bay sediments.

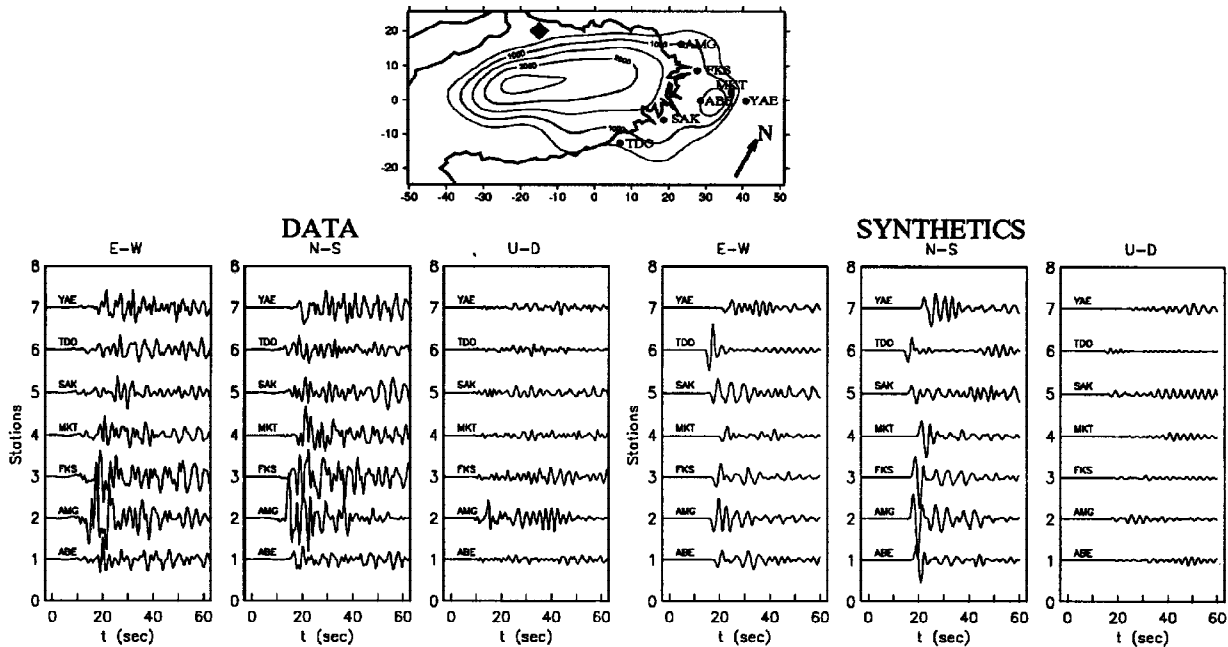


Fig. 2: The figure at the top represents a map of the Osaka bay, with the description of the bottom of the sedimentary layer. The diamond represents the location of the Kobe earthquake and the circles, the location of the CEORKA stations. Below the map, are represented the data and synthetics for each station and each component.

Our simulation allow us to interpret the large amplitude of the ground motion at some sites as basin-induced surface waves. We introduce the geometry of the basin using a sedimentary layer of velocity for the  $P$  wave 2 km/s and for the  $S$  wave of 1 km/s. The geometry of the bottom of the sedimentary layer is represented on the map of the Osaka Bay (T. Kagawa, personal communication) (Top of the Figure 2). Excellent quality broad-band records were obtained on stations *ABE*, *AMG*, *FKS*, *MKT*, *SAK*, *TDO* and *YAE* installed by the CEORKA (Committee of Earthquake Observation and Research in the Kansai Area, Toki95). The set of the observed seismograms are represented above the synthetics. The difference in the frequency content between data and synthetics is due to the choice of a source with a very smooth and centered spectrum. In fact the time story for the slip function was assumed Gaussian with a "characteristic" time of 3 sec (the classical Ricker pulse with three lobes is in fact proportional to the second derivative of the Gaussian). On the other hand, the discretisation of the basin imposes a sever limit in the frequencies that can be propagate. It is a kind of implicit filter.

From these preliminary results, we can notice that the large amplitudes, due to the amplification of the basin, especially clear on the observed seismograms at *AMG*, are well reproduced on synthetics. The large amplifications and the relative amplitudes among all the stations suggest that our simulation captures the essential physics of the problem. Our synthetics show relatively large basin-induced surface waves. These waves are of great interest as in many instances they may induce considerable damage. These encouraging results could be improved by introducing a more realistic bilateral rupture process, well defined now by many authors.

## INCIDENCE OF PLANE $SH$ WAVES IN THE MEXICO CITY BASIN

We also used the VPM to evaluate the 3D seismic response on the surface of a simplified model of the Mexico City basin. We considered the irregular 3D structure formed by the uppermost strata of highly compressible high water content clay, underlaying by a deeper, much harder structure.

We considered a homogeneous irregular layer with  $S$  wave velocity of  $\beta_R = 0.1$  km/sec (although in some particular sites this velocity is as low as 35 m/sec) and a Poisson ratio of 0.495. These values agree well with those reported recently for the static and dynamic behavior of the Mexico City clay sediments (e.g., Centro de Investigación Sísmica, 1994). Thus,  $P$  wave velocity is about  $\alpha_R = 1$  km/s.  $S$  wave velocity for the surrounding material was estimated to be 3.0 km/s. To take into account the seismic waves attenuation in the basin a quality factor  $Q = 25$  was used in the computations. This value corresponds to the one obtained from several *insitu* measurements on the soft clayed strata of Texcoco Lake.

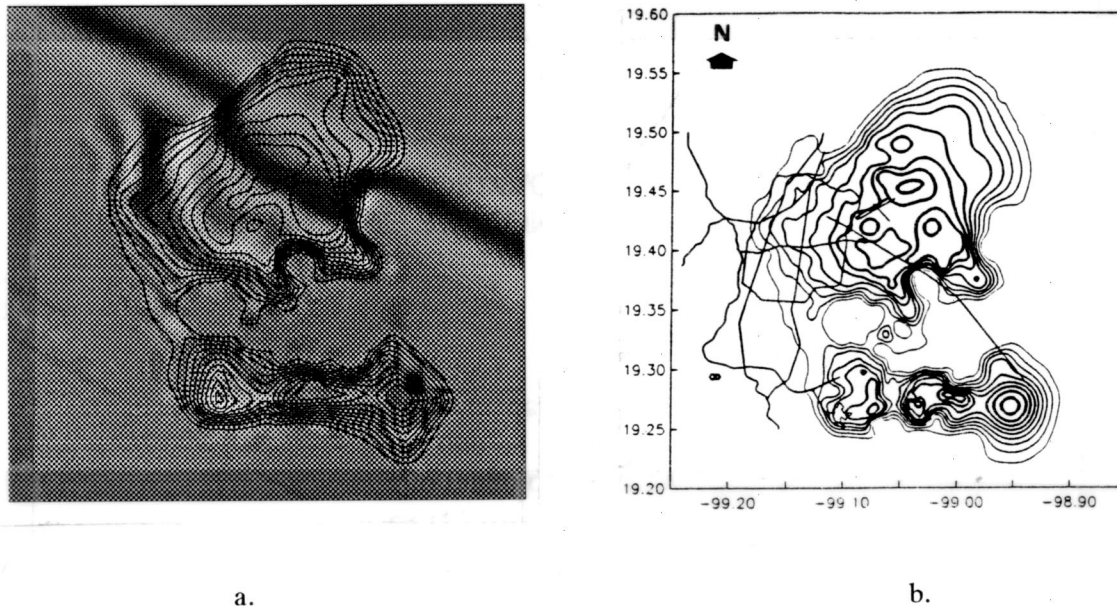


Fig. 3: Model of the Mexico Valley (a.) and the simulation using VPM method (b.).

The 3D irregular geometry in our computations was inferred from the detailed zonation of Mexico City and from the precise knowledge of the fundamental period ( $T_0$ ) distribution. Therefore, with the average  $S$  wave velocity (0.1 km/s), the depth distribution in the geometry was obtained using the theoretical relation  $h = \beta_R T_0 / 4$ . Figure 3a illustrates contours of depth distribution in the 3D model under study, the southern minima corresponds to the sediments from the Chalco and Xochimilco Lakes, whereas the large extension to the north corresponds to the ancient Texcoco Lake sediments. The size of the grid is 40.96 x 40.96 km and it was sampled using 256 x 256 nodes, with a grid spacing of 0.16 km. The very low  $S$  wave velocity of the uppermost sediments and the selected discretization imposes severe limits upon the observable wavelength ( $\lambda \geq 0.5$  km) or, in other terms, the maximum frequency is then  $f_{max} = \beta_R / \lambda \leq 0.2$ . Because of the large lateral extension of the model the 1D solution is computed and it is the reference value.

We assumed an incident plane  $SH$  wave arriving at the base of the 3D irregular model for the Mexico City basin, with an incident angle  $\gamma = 60^\circ$  with respect to the vertical and azimuth of  $\phi = 30^\circ$ . The waveform of the incoming motion was given by a Ricker's wavelet with characteristic period  $t_p = 2$  sec. We computed synthetic displacements at the surface of the model. Figure 3b displays a snapshot for the  $E - W$  component. Despite the small useful frequency range (up to about 0.25 Hz), our simulation shows dynamic effects not computed before. The larger effects appear to occur at the deeper part of model (a spot corresponding to the Texcoco Lake zone). Our calculations show a clear delay in the wavefront evolution. The spatial distribution of peak ground motion can be correlated with both the basin shape and the azimuth. This is yet to be accomplished and is investigated now.

## CONCLUSION

The presented results show the feasibility of the VPM to simulate the seismic response of large-scale shallow sedimentary basins. The preliminary results are encouraging and suggest the VPM can help to explain and quantify the basin-induced surface waves. The method is still in development stage. To uncover the advantages and limitations of this technique will require further scrutiny.

## ACKNOWLEDGEMENT

Thanks are given to J. Bielak, E. Faccioli and R. Geller for their useful suggestions. Their works provided inspiration to formulate the method presented here. This work was initiated while F.J. Sánchez-Sesma visited DPRI of Kyoto University, Japan. Part of the computations were done at the CRAY-YMP of UNAM, México. This work was partially supported by the Japanese Society for the Promotion of Science, by DGAPA of UNAM, México, under grant IN108295, by CONACYT, México, by Secretaría General de Obras del DDF, México and by Cray Research Inc., under Grant SC-100894.

## REFERENCES

- Aki, K. (1988). *Local site effects on strong ground motion*, pages 103–155. Am. Soc. Civil Engr., Geotechnical Special Publication No. 20.
- Avila-Carrera, R., Suárez, M., and Sánchez-Sesma, F.J. (1993). Simulación de la propagación de ondas sísmicas en configuraciones irregulares con un método pseudospectral. pages 182–189. X Mexican National Conf. Earth. Eng., Puerto Vallarta, Mexico.
- Faccioli, E., Maggio, F., Quarteroni, A., and Tagliani, A. (1996). *Spectral domain decomposition methods for the solution of acoustic and elastic wave equations*, page in press.
- Frankel, A. (1993). Three-dimensional simulation of seismic waves in the Santa Clara valley, California, from a Loma Prieta aftershock. *Bull. Seism. Soc. Am.*, 83:1020–1041.
- Geller, R.J., Hara, T., and Tsuboi, S. (1990). On the equivalence of two methods for computing partial derivatives of seismic waveforms. *Geophys. J. Int.*, 100:153–156.
- Geller, R.J. and Ohminato, T. (1994). Computation of synthetic seismograms and their partial derivatives for heterogeneous media with arbitrary natural boundary conditions using the Direct Solution Method. *Geophys. J. Int.*, 116:421–446.
- Geller, R.J. and Hatori, T. (1995). DSM synthetic seismograms using analytical trial functions: plane-layered, isotropic, case. *Geophys. J. Int.*, 120:163–172.
- Luco, J.E., Wong, H.I., and De Barros, F.C.P. (1990). Three-dimensional response of a cylindrical canyon in a layered half-space. *Earthq. Engrg. Structl. Dyn.*, 19:799–817.
- Martínez, B. and Bielak, J. (1980). On three-dimensional seismic response of earth structures. volume 8, pages 523–530. 7th World Conf. on Earthq. Eng., Istanbul, Turkey.
- Olsen, K.B., Archuleta, R.J., and Matarrese, J.R. (1995). Three-dimensional simulation of a magnitude 7.75 earthquake on the san andreas fault. *Science*, 270:1628–1632.
- Pérez-Rocha, L.E., Sánchez-Sesma, F.J., and Reinoso, E. (1991). Three-dimensional site effects in Mexico city: evidences from accelerometric network observations and theoretical results. pages 327–334. 4th Intl. Conf. on Seismic Zonation, Stanford, California August 25-29, Vol II.
- Perrot, J., Sánchez-Sesma, F.J., Irikura, K., Rodríguez-Zúñiga, J.L and Avila-Carrera, R. (1995). Simulation of the seismic response of Osaka basin during the January 17, 1995 Kobe earthquake using the Variational Projection Method. AGU Fall meeting, San Francisco.
- Rodríguez-Zúñiga, J.L. and Sánchez-Sesma, F.J. (1996). *Seismic response of the Mexico City valley: A new approach*, in preparation.
- Sánchez-Sesma, F.J. (1987). Site effects on strong ground motion. *Int. J. Earthquake Eng. Struct. Dyn.*, 6:124–132.
- Sánchez-Sesma, F.J., Ramos-Martínez, J., and Campillo, M. (1993). An indirect boundary element method applied to simulate the seismic response of alluvial valleys for incident P, S and Rayleigh waves. *Earthq. Engrg. Structl. Dyn.*, 22:279–295.
- Sánchez-Sesma, F.J. and Luzón, F. (1995). Seismic response of three-dimensional alluvial valleys for incident P, S and Rayleigh waves. *Bull. Seism. Soc. Am.*, 85:269–284.